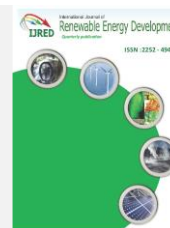




Contents list available at IJRED website

**International Journal of Renewable Energy Development**

Journal homepage: <https://ijred.undip.ac.id>



Research Article

# Solar Tracking System with Photovoltaic Cells: Experimental Analysis at High Altitudes

Elmer Rodrigo Aquino Larico<sup>a\*</sup> and Angel Canales Gutierrez<sup>a,b</sup>

<sup>a</sup>Doctorado en Ciencia Tecnología y Medio Ambiente, Escuela de posgrado, Universidad Nacional del Altiplano de Puno, Perú

<sup>b</sup>Facultad de Ciencias Biológicas, Programa de Ecología de la Universidad Nacional del Altiplano de Puno, Perú

**Abstract.** There is currently an urgent need to study the application of solar energy to photovoltaic systems due to the need to produce electricity; indeed, maximizing the performance of solar energy promotes efficient and sustainable energy systems. The objective of this study was to determine the photovoltaic performance of a dual-axis solar tracker based on photovoltaic cells with different inclination angles at high altitudes above 3800 m.a.s.l. A solar tracking system activated by two linear actuators was implemented to automatically follow the trajectory of the sun during the day, and the results were compared with those from a fixed photovoltaic system. In addition, due to the climatic variation in the area, photovoltaic cells installed at different inclination angles were used to maximize electricity production and processed by a programmable logic controller (PLC). Finally, principal component analysis (PCA) was used to determine the factors that influenced the performance of the photovoltaic system during the experimental period. The results showed that the maximum monthly performance of the solar tracker was 37.63% greater than that of the fixed system, reaching 10.66 kWh/m<sup>2</sup>/d on sunny days in peak sun hours (PSH). On days with frequent rain and clouds, the partial yield was less than 14.38%, with energy production during PSH of 6.54 kWh/m<sup>2</sup>/d. Therefore, in this high-altitude area, the performance of the solar tracker was greater from July to October; from November to February, the performance was reduced due to the occurrence of rain.

**Keywords:** Photovoltaic cell, solar irradiation, solar tracker, photovoltaic efficiency.



@ The author(s). Published by CBIORE. This is an open access article under the CC BY-SA license (<http://creativecommons.org/licenses/by-sa/4.0/>)

Received: 26<sup>th</sup> Dec 2021; Revised: 25<sup>th</sup> March 2022; Accepted: 6<sup>th</sup> April 2022; Available online: 17<sup>th</sup> April 2022

## 1. Introduction

Renewable energy comes from natural sources or environmental resources and has recently undergone accelerated growth due to local availability (Sharma *et al.*, 2021). Sources of sustainable energy production, such as solar, wind, hydroelectric, biomass and geothermal energy, could reduce carbon emissions (Suki *et al.*, 2022) and gas emissions that affect the environment (Ni & Kurita, 2020). Solar energy is one of these energies and has potential for application in thermal concentration and electricity production in photovoltaic systems (Hua *et al.*, 2019).

Solar energy is widely applied in photovoltaic systems due to its availability and cost, which is reduced because it does not require fossil fuel to function; furthermore, solar energy systems require simple maintenance, are easy to install and are beneficial for the environment (Joshi *et al.*, 2022). Photovoltaic solar panels have a yield of less than 40%, depending on the type of solar panel, the solar irradiance of the area, the geographical location and other factors, such as solar tracking systems (Lai & McCulloch, 2017).

Photovoltaic systems convert sunlight into electricity; however, to improve the capture of solar irradiation, they use cooling techniques on the surface of the module, maximum power point tracking (MPPT) with a regulator

or solar tracking systems (Ocloñ *et al.*, 2020). Thus, the energy produced by a photovoltaic module increases the performance of the system (Du *et al.*, 2021). In this way, these strategies, including the use of solar trackers, allow the capture of more solar radiation by maintaining the surface of the module approximately perpendicular to the source for a longer period (Seme *et al.*, 2017).

In this sense, single-axis and double-axis solar tracking systems maximize electricity production, increasing the capture of solar radiation and photovoltaic efficiency by between 15% and 45% compared to other fixed photovoltaic systems of equal power (Soulayman *et al.*, 2021); by 19.97% compared with dual-axis systems based on light-dependent resistors (LDR) (Jamroen *et al.*, 2021); by up to 40% compared with other low-cost systems with four and 8 simulated LDRs (Pawar *et al.*, 2021); and by up to 54.39% compared to using a closed circuit control loop (Fuentes-Morales *et al.*, 2020). Currently, dual-axis solar trackers have greater photovoltaic efficiency in the production of electricity because they follow the trajectory of the sun in a synchronized movement across the horizontal and vertical axes with different control algorithms (Motahhir *et al.*, 2020). One of the important aspects of two-axis solar trackers is that they can follow the trajectory of the sun in any direction by means of motors or actuators, making their operation more precise (Sidek *et al.*, 2017).

\* Corresponding author  
Email: [eaquinol@unap.edu.pe](mailto:eaquinol@unap.edu.pe) (E.R.A. Larico)

To control a solar trajectory tracking system, several control strategies are used, including open, closed or combined loops (Fuentes-Morales et al., 2020) Classic strategies such as ON-OFF, PI and PID controls are also used; in addition, control algorithms are implemented through a programmable logic controller (PLC), software for entering information about the sensors, the sequence of the processes and the output of the actuators that automatically direct the solar tracker (Mao et al., 2018). Therefore, some solar trackers use photosensors or photodiodes as the main solar tracking device; however, the normal operation of these sensors depends on clear skies and favourable weather conditions (Su et al., 2018). Others have used low-cost LDRs (Hoffmann et al., 2018) and photovoltaic panels (Kivrak, 2013). In addition, the performance of these solar trackers can be improved by MPPT strategies (Kumar et al., 2020).

The performance of trackers is affected by several factors, such as irregular precipitation, partial cloud cover, and seasonality. To correlate these variables in a scatter plot, PCA is used to determine which factor influences the loss of performance (Yang et al., 2017). This technique divides the variables into relevant blocks and is very effective for the monitoring and detection of faults (Bakdi & Kouadri, 2018).

However, in the Peruvian Altiplano with elevated altitudes above 3800 m.a.s.l., there are no studies of solar tracking systems that can operate on sunny days that are partially cloudy and have heavy rains. Moreover, low-cost sensors (e.g., LDRs) (Bharati et al., 2017; Imhade et al., 2018) could be affected by climatic variation and the accumulation of dust in the tracking of the sun's trajectory. For this reason, the use of solar trackers based on photovoltaic cells is proposed because these cells have high resistance to climatic variation and sudden changes in temperature and light and heavy precipitation, sometimes including hail, and irregular partial shading. In addition, photovoltaic efficiency was analysed by PCA to determine which factors influenced the production of electricity in solar trackers.

Therefore, the objective of this research was to determine the photovoltaic performance of a dual-axis solar tracker with photovoltaic cells at different inclination angles and high altitudes above 3800 m.a.s.l.



Fig. 1 Geographical location of the Peruvian Altiplano

## 2. Materials and Methods

### 2.1 Location

The study was conducted in the Peruvian Altiplano, at an altitude of 3825 m.a.s.l., in the southern hemisphere. The south latitude of the study site is  $-15^{\circ}29'27''$  and the west longitude is  $-70^{\circ}07'37''$ , and the area was formed largely by irregular geography (Figure 1). The temperature ranges from  $4^{\circ}\text{C}$  to  $10^{\circ}\text{C}$ , with a mean annual maximum temperature of  $18.08^{\circ}\text{C}$  and a mean annual minimum temperature of  $-7.5^{\circ}\text{C}$ . The research process was carried out from July 2021 until February 2022 at the National University of the Altiplano, Peru.

### 2.2 Mechanical structure, linear actuators and solar tracker prototype

To perform this research, a solar tracker with two axes of movement was implemented. The first axis is located in the central part of the support (steel tube) in a vertical position; it was machined with a 3" diameter double bearing to prevent breakage of the axis. The second axis is located in the upper part of the vertical support; it is mechanized, with a horizontal axis that supports the structural base and the 100 W monocrystalline photovoltaic module. Both axes were driven by two linear actuators (ECO-WORTHY) with a load capacity of 330 lb, stroke of 355 mm, and a travel speed of 5.7 mm/s.

The linear actuator of the first axis follows the path of the sun from east to west, and the linear actuator of the second axis moves from north to south. Finally, both mechanisms were controlled by PLC Model 1214C (S7-1200 SIEMENS) with high precision. The mechanical structure of the solar tracker is shown in Figure 2.

The prototype of the solar tracker was machined with steel tubes 4" and 3" in diameter, with a thickness of 2 mm so that it was resistant to wind and rain. In the central part, the linear actuator was located in the horizontal position for east to west movement; from the middle of the support to the top of the tracker, the linear actuator was located in a vertical position for north to south movement.

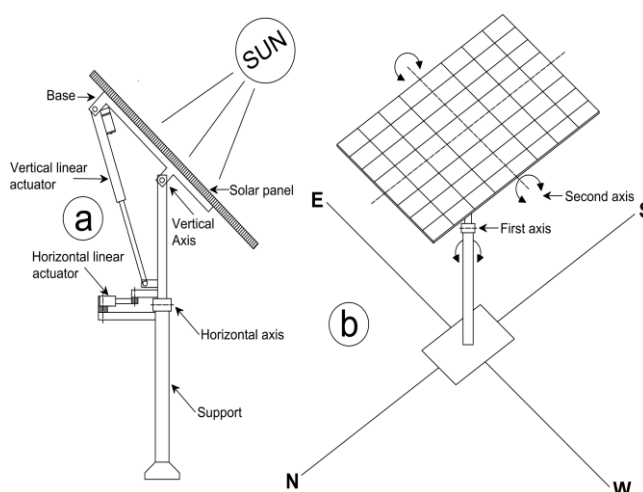


Fig. 2 Solar tracker: (a) mechanical structure with linear actuators, (b) tracking of the first and second axes of rotation

### 2.3 Solar irradiance sensor for the solar tracking system

To optimize the capture of solar irradiance, five 3 W photovoltaic cells oriented to the north with different inclination angles (0°, 4°, 15°, 26°, 30°) were used, taking the latitude of the area as the central point, as determined by the central composite design (response surface method) (Yu *et al.*, 2019). The reasoning for this design is expressed by the design centre (0), the design radius and the decoded equation for (-1 and +1) and the minimum and maximum extremes (-α and +α), expressed in Equations (1), (2) and (3), respectively.

$$Z_{j(0)} = \frac{Z_{j(max)} + Z_{j(min)}}{2} \tag{1}$$

$$\Delta Z_j = \frac{Z_{j(max)} - Z_{j(min)}}{2} \tag{2}$$

$$Z_j = Z_{j(0)} + \left( \frac{X_j}{\alpha} \Delta Z_j \right) \tag{3}$$

Table 1 shows the inclination angles of the photovoltaic cells determined by the central composite design.

Where  $Z_{j(0)}$  is the centre of the design (15°),  $Z_{j(max)}$  and  $Z_{j(min)}$  are the extremes (0° and 30°),  $\Delta Z_j$  is the radius of the design,  $X_j$  and  $\alpha$  are the coded variables, finally  $Z_j$  are the intermediate levels (4° and 26°).

The photovoltaic cells were calibrated by a solar metre SOLAR-100 (AMPROBE-USA), which was used as a solar irradiance sensor. Each photovoltaic cell measures the solar irradiance independently connected to the PLC; within its programming, the PLC obtains the maximum reference solar irradiance value and compares it with the irradiance of the solar tracker to optimize the range of motion of the axes and find the point of maximum power.

In the Peruvian Altiplano, the winter season is the coldest season, during which the sun moves farther away and the angle of inclination of the surface of the photovoltaic cell is greater; in the summer season, the solar rays are approximately perpendicular to the surface of the earth and the photovoltaic cells have a lower angle of inclination, thus maximizing the capture of solar irradiation (Figure 3).

### 2.4 PCA of photovoltaic systems and scaling of photovoltaic cells

To determine the differences in energy production during PSH, on sunny days with rain, and considering the variation in the temperature of the area, we used the statistical technique principal component analysis (PCA) (Kazem *et al.*, 2022). Compared with another 100 W fixed monocrystalline photovoltaic system inclined at 15°, the difference in the generation of electricity was determined. The data were processed by InfoStat software according to the statistical design.

In the scaling of photovoltaic cells, the short circuit current of a cell is directly proportional to the solar irradiance, so that if the terminals of the photovoltaic cell are short-circuited, both currents are equal, having a direct relationship with the current short circuit of the photovoltaic cell and solar irradiance. In this way, the current transducer standardizes the current at (4 to 20 mA, connected to the analogue input of the PLC (Figure 4) processed with the ladder programming language, according to the IEC-61131-3 standard (Commission, 2009). The PLC converts the electric current to a digital signal with a range of (0 to 20000) in integers (INT) before finally scaling it to solar irradiance (W/m<sup>2</sup>) in real numbers (Figure 5). Solar irradiation data were taken every 20 seconds from 6:00 a.m. to 6:00 p.m.

**Table 1**  
Angle of inclination of the photovoltaic cells by means of the central composite design.

Inclination angle of the cells	Factor symbol			Levels			
	Dec	Code	-α	-1	0	+1	+α
Level	X1	A	-1.41	-1	0	+1	+1.41
Degrees (°)	X2	B	0	4	15	26	30

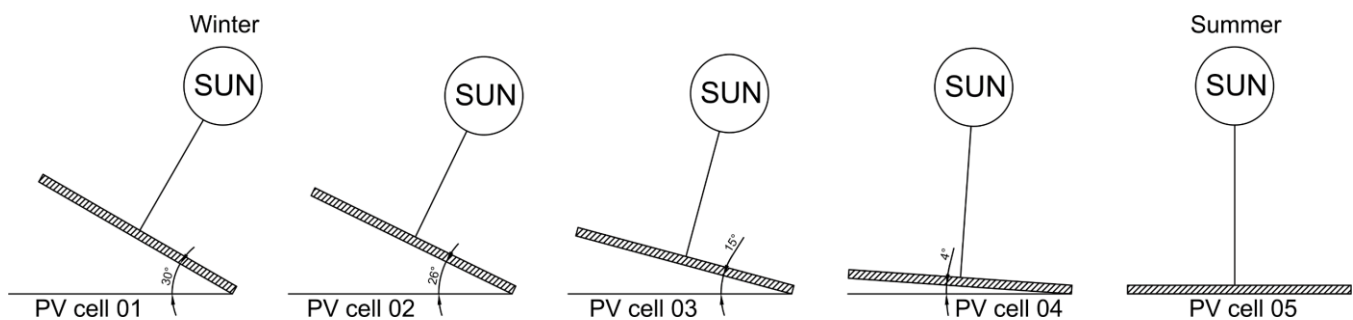


**Fig. 3** Photovoltaic cells at different inclination angles

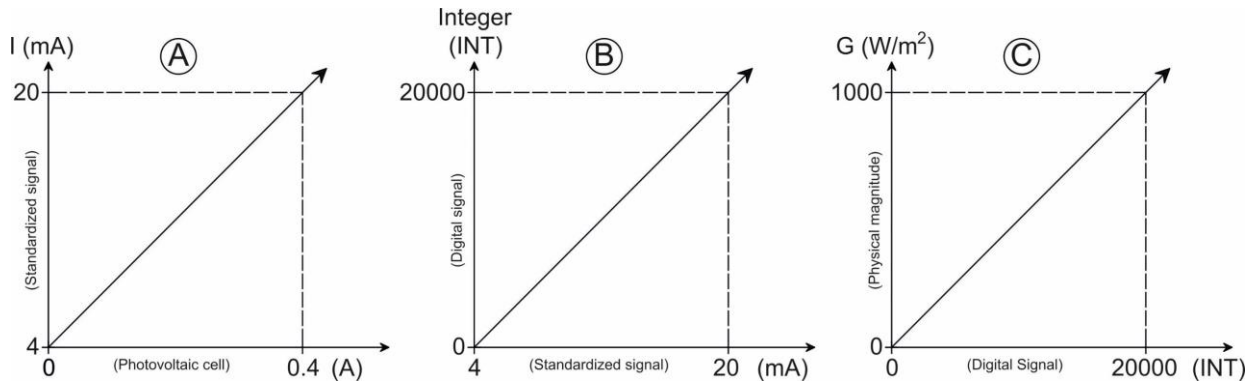


**Fig. 4** Scaling of electrical signals to digital signals: (A) current to normalized signal, (B) normalized signal to integers, and (C) integers to physical magnitude

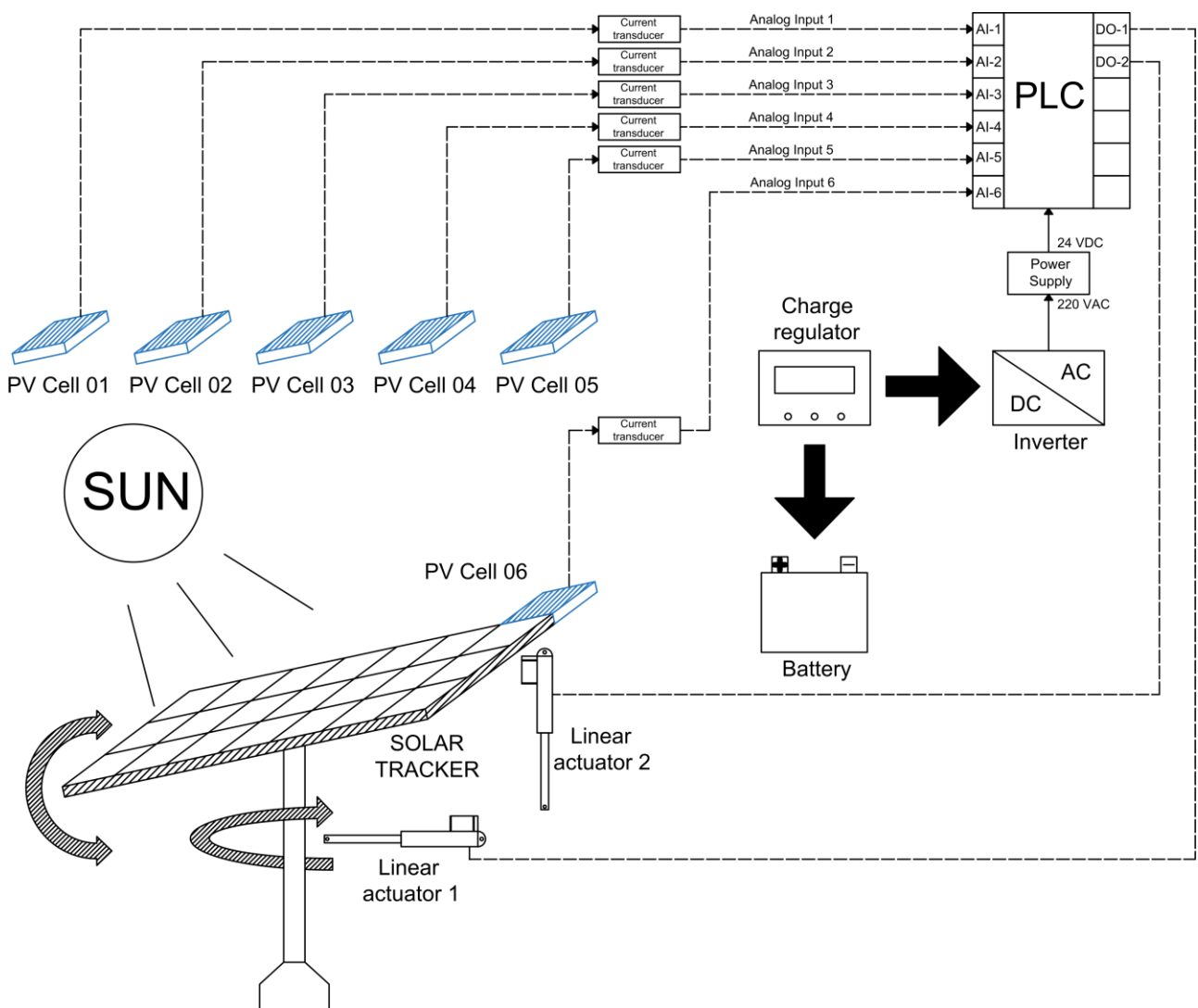


**Fig. 5** Diagram of the electrical connections of the solar tracker

*2.5 Solar tracker control system*

The control system of the solar tracker was implemented by a PLC (S7-1200 SIEMENS). This controller was in charge of processing the analogue inputs

of the solar irradiance sensors, the process capturing the maximum amount of solar irradiance, the automatic control of the solar tracker and the outputs for the control of the linear actuators. The control strategy was implemented in the PLC with the ladder programming

language. This control strategy allowed the search for the maximum solar irradiance of the five photovoltaic cells installed at different inclination angles, comparing them with the photovoltaic cells of the solar tracker to find the point of maximum power. The control algorithm of the solar tracker is shown in Figure 6.

Figure 7 shows the initial position of the solar tracker being approximately perpendicular to the ground and facing east, following the sun during the day, finally ending with an almost perpendicular position facing west at 18:00 h. The solar panel is inclined to an approximate angle of 15° to protect the linear actuators from possible rain. Finally, at 06:00 h, it returns to its initial position. However, on partially cloudy days with a solar irradiance lower than 400 W/m<sup>2</sup>, the system is blocked, preventing the solar tracker from performing a search. This function of tracking the maximum point of solar irradiance was performed as a function of time programming (Nuwayhid *et al.*, 2001), following the trajectory of the sun every 15 minutes from 08:00 h to 16:00 h.

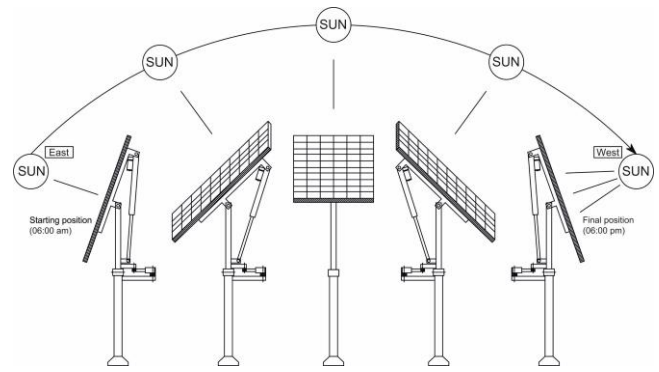


Fig. 7 Initial and final positions of the solar tracker

### 2.6 Performance evaluation of photovoltaic generation

The gain in electricity production is determined by the difference in the solar tracker and the fixed system, as shown in Equation (4) (Jamroen *et al.*, 2020).

$$\Delta E = \frac{E_{tracking} - E_{fixed}}{E_{fixed}} \times 100\% \tag{4}$$

where  $\Delta E$  is the relative percentage difference (%).  $E_{tracking}$  is the energy generated by the solar tracker in (Wh), and  $E_{fixed}$  is the energy generated by the fixed system in (Wh).

## 3. Results and discussion

### 3.1 Analysis of the photovoltaic performance of the solar tracker compared to that of the fixed photovoltaic system

During the experimental period (Figure 8), the solar tracker obtained the maximum energy production during PSH with 10.66 kWh/m<sup>2</sup>/d compared to the fixed photovoltaic system, which produced 7.75 kWh/m<sup>2</sup>/d, representing 37.63% more efficiency in August due to the occurrence of sunny days. However, in December, the lowest energy production was recorded, with 6.54 kWh/m<sup>2</sup>/d for the solar tracker during PSH and 5.72 kWh/m<sup>2</sup>/d for the fixed photovoltaic system, representing 14.38% more efficiency. The reduction in energy was due to the high rainfall, with a monthly average of 90 mm/month, and partially cloudy days. Finally, in PSH during the experimental period, the energy production of the solar tracker was 8.30 kWh/m<sup>2</sup>/d and that of the fixed system was 6.75 kWh/m<sup>2</sup>/d, representing 22.85% more electricity production. The reduction in efficiency was due to the climatic variation in the Peruvian Altiplano, with the occurrence of rainy days, especially from December to February, and partially cloudy and sunny days. According to Yilmaz *et al.* (2015), the energy produced by a dual-axis tracking system was 55.91 Wh, while that produced by a fixed system was 41.71 Wh, with the former generating 34.02% more energy generation.

Therefore, the solar tracker produces more energy than the fixed system on sunny days; however, on partially cloudy and rainy days, the performance is similar between the two systems. In addition to the high altitude, the photovoltaic cells showed good performance with climatic variation. Other authors have mentioned that the latitude of an area influences the photovoltaic performance of these systems (Bahrami *et al.*, 2016; Tan *et al.*, 2019). In

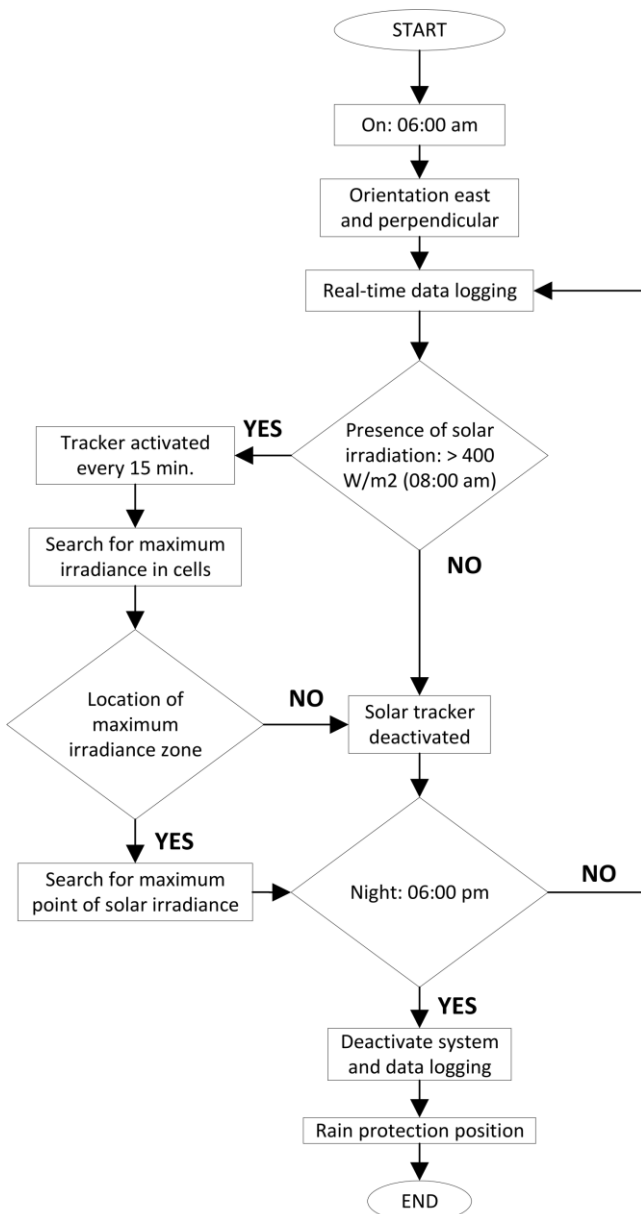


Fig. 6 Control algorithm of the solar tracking system

addition, an experimental study of an intelligent closed-loop solar tracker implemented in an urban area showed a yield of 30.10% (Kang *et al.*, 2019), similar to the results obtained in this study at high altitudes. Moreover, dual-axis solar tracking systems improve photovoltaic performance by between 30% and 45% due to the different types of control algorithms or programming languages implemented (Singh *et al.*, 2018) Therefore, these performance results were close to those of this study.

### 3.2 Solar irradiance curve analysis

The solar irradiance curve in the Peruvian Altiplano at high altitude has an irregular behaviour due to the varied climatic conditions of the area; from July to October, there is a high solar irradiance above 1000 W/m<sup>2</sup> because these months are sunny months, while the solar irradiance is reduced from November to January due to the occurrence of rain and partially cloudy days. Moreover, in February, the solar irradiance curve was very low due to high amounts of precipitation (118 mm/month) and partially cloudy days with solar irradiance below 1000 W/m<sup>2</sup> (Figure 10). In this sense, this high-altitude region is characterized by a rainy season that begins in October and ends between March and April. This climatic variation affects the solar irradiance captured by photovoltaic systems, reducing photovoltaic yield. Therefore, the performance of the solar tracker was better between July and October and reduced between December and February; therefore, in these months, the fixed photovoltaic system would be the best option.

### 3.3 Effect of tilt angle of photovoltaic cells through response surface design

The effects of tilt angles on the surface of the photovoltaic cells were analysed using the response surface design. Of the factors studied, the tilt angles are significant ( $p < 0.0433$ ), explaining that this variation influences the capture of solar irradiance in the solar tracking system, so the relationship between the variables and the response are shown in Figure 9. The response surface is concave downwards showing the interaction between the factors to maximize the capture of solar irradiation, obtaining the maximum efficiency of the photovoltaic cells in the production of electricity, therefore,

the response surface generated validates the angles obtained.

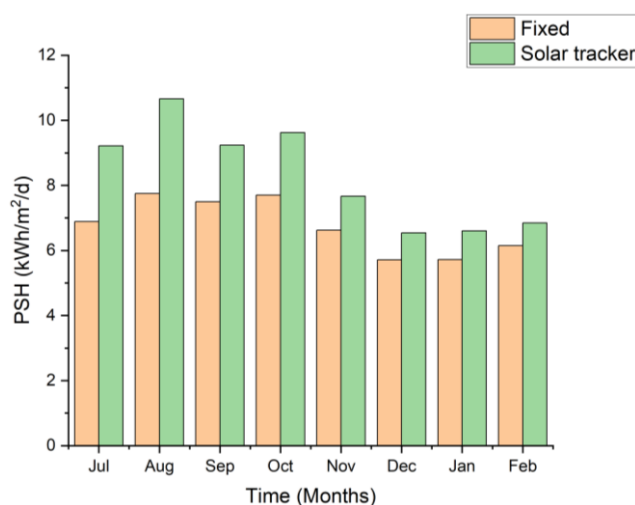


Fig. 8 Monthly energy production of the solar tracker compared to the fixed photovoltaic system

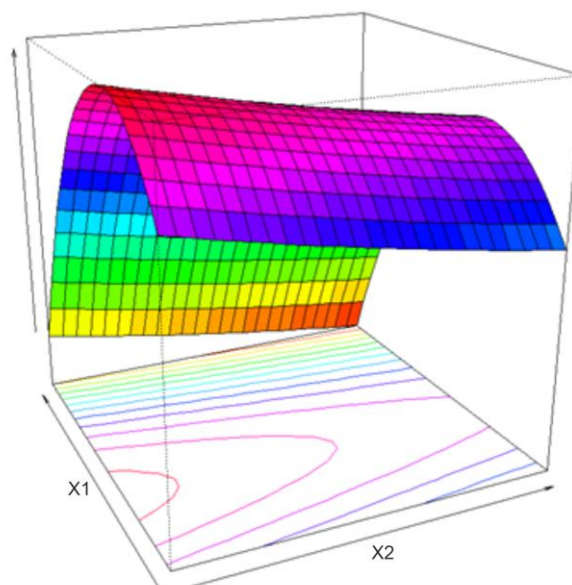


Fig. 9 Response surface, effect of the tilt angles of the photovoltaic cells

Table 2 PSH and climatic variables of the solar tracker and the fixed system (2021-2022).

Month	Fixed PSH	PSH tracker	Precipitation	Ambient temperature	
	kWh/m²/d		mm/month	Max.	Min.
July	6.89	9.21	1.80	15.80	-7.80
August	7.75	10.66	5.10	16.70	-6.10
September	7.50	9.23	22.50	17.40	-1.90
October	7.70	9.62	42.80	18.60	-0.40
November	6.62	7.67	49.60	18.80	1.00
December	5.72	6.54	90.00	17.50	2.60
January	5.72	6.60	118.00	16.60	3.20
February	6.14	6.85	104.00	16.50	3.40

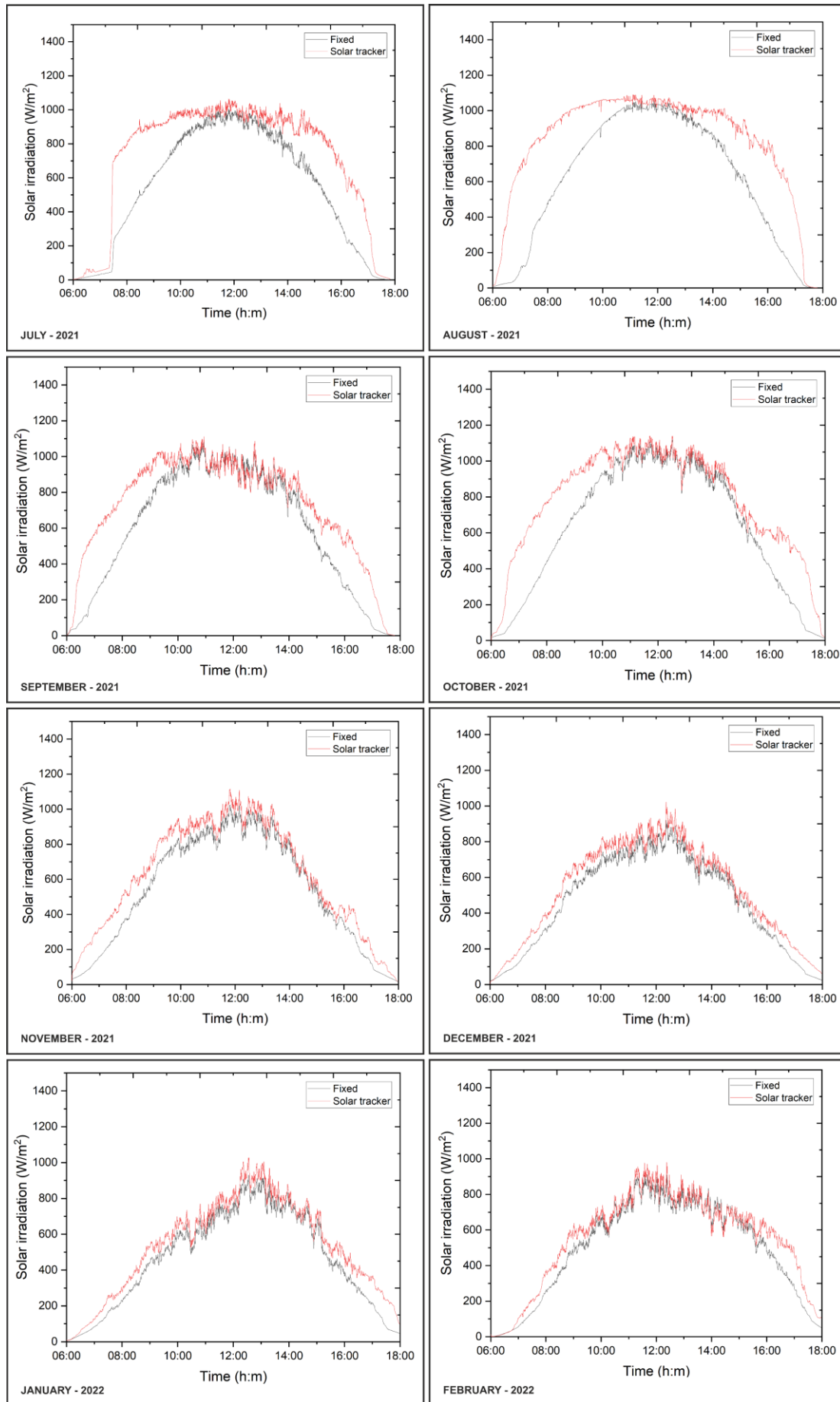
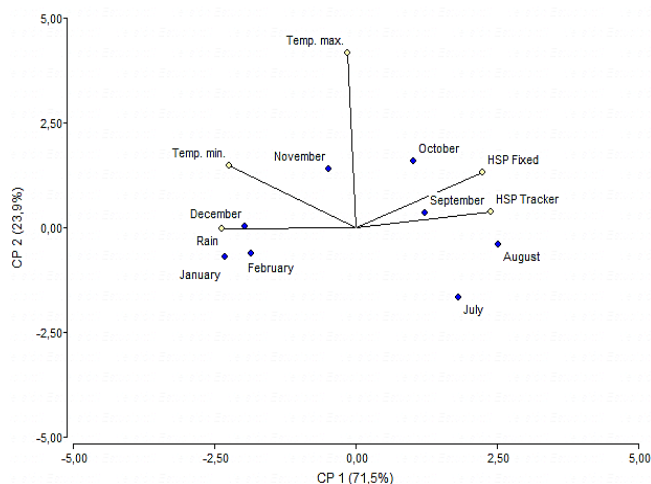


Fig. 10 Solar irradiance curves between July and February 2022.



**Fig. 11** PCA for the solar tracker and the fixed photovoltaic system.

### 3.4 Behaviour of the photovoltaic yield according to PCA

The energy production by the fixed system and the solar tracker and temperature and precipitation variables for the area from July 2021 to February 2022 are shown in Table 2. The results of the PCA shown in Figure 11 demonstrate that the greatest captures of solar irradiation for the solar tracker and the fixed system were from July to October (with sunny days); in contrast, from December to February, electricity production was lower due to the occurrence of rainfall and precipitation ranging between 49.60 mm/month and 118 mm/month, which was associated with low temperatures. Principle component 1 (PC 1) explained 71.50% of the variation in the model, considering that rainfall affects the production of energy by the solar tracker and fixed photovoltaic systems during PSH, while PC 1 and PC 2 explain 95.40% of the variation in the model by accounting for the low temperatures in the reduction in the photovoltaic yield. However, although rainfall reduces photovoltaic performance, it also cleans the surface of the photovoltaic module, which is an important advantage that counteracts the accumulation of dust (Del Pero *et al.*, 2021).

### 3.5 Behaviour of photovoltaic cells and linear actuators

The photovoltaic cells implemented to measure the solar irradiance and installed at different inclination angles showed good resistance to the climatic variation in the area; however, the accumulation of dust on sunny days slightly reduced the capture of solar irradiance and the energy yield (El Shenawy & El El Ghetany, 2021) In contrast, strong rains cleaned the photovoltaic cells (Figure 12). Moreover, the linear actuators worked in optimal conditions because the drive motor was hermetically sealed, preventing the entry rainwater, and the stem was made of aluminium, presenting high resistance to corrosion.

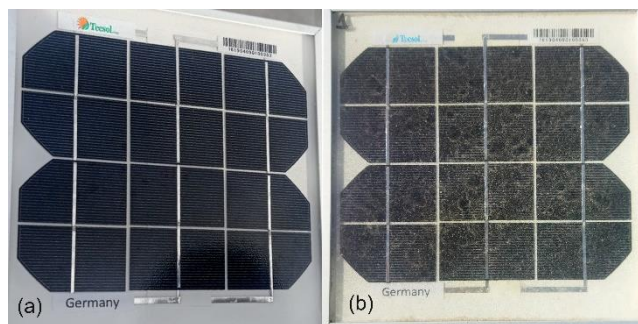


**Fig. 12** Photovoltaic cells: (a) clean photovoltaic cell, (b) photovoltaic cell with slight accumulation of wet dust

## 4. Conclusion

In the Peruvian Altiplano, the dual-axis solar tracker had a maximum monthly photovoltaic yield of 37.63% more than the fixed photovoltaic system, and the energy production during PSH was 10.66 kWh/m<sup>2</sup>/d more than that in the fixed system, which produced 7.75 kWh/m<sup>2</sup>/d. In contrast, on rainy days with partial cloudiness, the performance of both photovoltaic systems was reduced to 14.38%, more than other photovoltaic systems. However, the PCA determined that the presence of rain affects the capture of solar irradiation in the photovoltaic system; between July and October, there is greater energy production because there was a greater number of sunny days with very low levels of partial cloudiness.

Therefore, the solar tracking system is more efficient than the fixed system because the tracker constantly follows the path of the sun through the double axis control of the linear actuators and the irradiance signal sent by the photovoltaic cells. Inclined at different angles, these cells, are more robust and performed well in the presence of rain and with the accumulation of dust due to the climatic variation in the area. Finally, although rainfall reduced the total energy production, it also cleaned the surface of the photovoltaic module, which is a considerable benefit given the accumulation of dust on this surface.

## Acknowledgements

Elmer R. Aquino Larico acknowledges financial support from the (Concytec-Banco Mundial) project "Improvement and Expansion of the Services of the National Science Technology and Technological Innovation System" 8682-PE through its executing unit ProCience. The funding award contract is number 01-2018-FONDECYT/BM-PROGRAMAS for doctoral programs in strategic and general areas. Doctorate in Science, Technology and Environment, EPG of the National University of the Altiplano of Puno, Peru.

**Author Contributions:** A) A method based on photovoltaic cells is proposed to capture the maximum solar irradiance with a solar tracker due to the temporal climatic variation (e.g., the occurrence of rain) at high altitudes. (B) An experimental study was performed at high altitudes above 3800 m.a.s.l. and PCA was performed to assess the findings. (C) A PLC was used to control the solar tracker and for data processing and to adjust the resistance of the linear actuators in response to sudden changes in climate.

**Funding:** This research was funded by (Concytec-World Bank), ProCiencia.

**Conflicts of Interest:** The authors declare no conflict of interest.

## References

- Bahrami, A., Okoye, C. O., & Atikol, U. (2016, 2016/09/01/). The effect of latitude on the performance of different solar trackers in Europe and Africa. *Applied Energy*, 177, 896-906. <https://doi.org/https://doi.org/10.1016/j.apenergy.2016.05.103>
- Bakdi, A., & Kouadri, A. (2018). An improved plant-wide fault detection scheme based on PCA and adaptive threshold for reliable process monitoring: Application on the new revised model of Tennessee Eastman process. *Journal of Chemometrics*, 32(5), e2978.
- Bharati, M., Divyakumari, R., & Swamy, B. (2017). Solar power tracking system and power saving in highway street light. *Int J Innov Res Comput Commun Eng*, 5(4), 276-285.
- Commission, I. E. (2009). Programmable Logic Controllers—Part 3: Programming Languages. *IEC Standard*, 61131-61133.
- Del Pero, C., Aste, N., & Leonforte, F. (2021, 2021/12/01/). The effect of rain on photovoltaic systems. *Renewable Energy*, 179, 1803-1814. <https://doi.org/https://doi.org/10.1016/j.renene.2021.07.130>
- Du, X., Li, Y., Wang, P., Ma, Z., Li, D., & Wu, C. (2021, 2021/01/01/). Design and optimization of solar tracker with U-PRU-PUS parallel mechanism. *Mechanism and Machine Theory*, 155, 104107. <https://doi.org/https://doi.org/10.1016/j.mechmachtheory.2020.104107>
- El Shenawy, E. T., & El El Ghetany, H. (2021). Effect of Dust Accumulation on the Performance of PV Modules under Cairo Climate Conditions. *International Journal of Renewable Energy Research (IJRER)*, 11(3), 1313-1321.
- Fuentes-Morales, R. F., Diaz-Ponce, A., Peña-Cruz, M. I., Rodrigo, P. M., Valentín-Coronado, L. M., Martell-Chavez, F., & Pineda-Arellano, C. A. (2020, 2020/12/01/). Control algorithms applied to active solar tracking systems: A review. *Solar Energy*, 212, 203-219. <https://doi.org/https://doi.org/10.1016/j.solener.2020.10.071>
- Hoffmann, F. M., Molz, R. F., Kothe, J. V., Nara, E. O. B., & Tedesco, L. P. C. (2018, 2018/01/01/). Monthly profile analysis based on a two-axis solar tracker proposal for photovoltaic panels. *Renewable Energy*, 115, 750-759. <https://doi.org/https://doi.org/10.1016/j.renene.2017.08.079>
- Hua, Z., Ma, C., Lian, J., Pang, X., & Yang, W. (2019). Optimal capacity allocation of multiple solar trackers and storage capacity for utility-scale photovoltaic plants considering output characteristics and complementary demand. *Applied Energy*, 238, 721-733.
- Imhade, O., Aderibigbe, A., & Elizabeth, A. (2018). Efficient and Low Cost Implementation of a Single Axis Solar Tracking System. *Journal of Electrical Engineering*, 18(2), 6-6.
- Jamroen, C., Fongkerd, C., Krongpha, W., Komkum, P., Pirayawaraporn, A., & Chindakham, N. (2021, 2021/10/01/). A novel UV sensor-based dual-axis solar tracking system: Implementation and performance analysis. *Applied Energy*, 299, 117295. <https://doi.org/https://doi.org/10.1016/j.apenergy.2021.117295>
- Jamroen, C., Komkum, P., Kohsri, S., Himananto, W., Panupintu, S., & Unkat, S. (2020, 2020/02/01/). A low-cost dual-axis solar tracking system based on digital logic design: Design and implementation. *Sustainable Energy Technologies and Assessments*, 37, 100618. <https://doi.org/https://doi.org/10.1016/j.seta.2019.100618>
- Joshi, S., Karamta, M., & Pandya, B. (2022, 2022/02/12/). Small scale wind & solar photovoltaic energy conversion system for DC microgrid applications. *Materials Today: Proceedings*. <https://doi.org/https://doi.org/10.1016/j.matpr.2022.01.461>
- Kang, H., Hong, T., Jung, S., & Lee, M. (2019, 2019/06/15/). Techno-economic performance analysis of the smart solar photovoltaic blinds considering the photovoltaic panel type and the solar tracking method. *Energy and Buildings*, 193, 1-14. <https://doi.org/https://doi.org/10.1016/j.enbuild.2019.03.042>
- Kazem, H. A., Yousif, J. H., Chaichan, M. T., Al-Waeli, A. H. A., & Sopian, K. (2022, 2022/01/01/). Long-term power forecasting using FRNN and PCA models for calculating output parameters in solar photovoltaic generation. *Heliyon*, 8(1), e08803. <https://doi.org/https://doi.org/10.1016/j.heliyon.2022.e08803>
- Kivrak, S. (2013). Design of a low cost sun tracking controller system for photovoltaic panels. *Journal of Renewable and Sustainable Energy*, 5(3), 033119.
- Kumar, K., Kiran, S. R., Ramji, T., Saravanan, S., Pandiyan, P., & Prabakaran, N. (2020). Performance evaluation of photovoltaic system with quadratic boost converter employing with MPPT control algorithms [Article]. *International Journal of Renewable Energy Research*, 10(3), 1083-1091. <https://www.scopus.com/inward/record.uri?eid=2-s2.0-85092188659&partnerID=40&md5=414f2168d0d4040d9889362eb98f80bf>
- Lai, C. S., & McCulloch, M. D. (2017). Levelized cost of electricity for solar photovoltaic and electrical energy storage. *Applied Energy*, 190, 191-203.
- Mao, K., Liu, F., & Ji, I. R. (2018). Design of ARM-based solar tracking system. 2018 37th Chinese Control Conference (CCC),
- Motahhir, S., El Hammoumi, A., & El Ghzizal, A. (2020). The most used MPPT algorithms: Review and the suitable low-cost embedded board for each algorithm. *Journal of Cleaner Production*, 246, 118983.
- Ni, B., & Kurita, K. (2020). The minimum wage, exports, and firm performance: Evidence from Indonesia. *Journal of Asian Economics*, 69, 101218.
- Nuwayhid, R., Mrad, F., & Abu-Said, R. (2001). The realization of a simple solar tracking concentrator for university research applications. *Renewable Energy*, 24(2), 207-222.
- Ocloń, P., Cisek, P., Kozak-Jagiela, E., Taler, J., Taler, D., Skrzyniowska, D., & Fedorczak-Cisak, M. (2020). Modeling and experimental validation and thermal performance assessment of a sun-tracked and cooled PVT system under low solar irradiation. *Energy Conversion and Management*, 222, 113289.
- Pawar, P., Pawale, P., Nagthane, T., Thakre, M., & Jangale, N. (2021, 2021/11/01/). Performance enhancement of dual axis solar tracker system for solar panels using proteus ISIS 7.6 software package. *Global Transitions Proceedings*, 2(2), 455-460. <https://doi.org/https://doi.org/10.1016/j.gltpr.2021.08.049>
- Seme, S., Srpčić, G., Kavšek, D., Božičnik, S., Letnik, T., Praunseis, Z., Štumberger, B., & Hadžiselimović, M. (2017). Dual-axis photovoltaic tracking system—Design and experimental investigation. *Energy*, 139, 1267-1274.
- Sharma, A., Dharwal, M., & Kumari, T. (2021, 2021/10/08/). Renewable energy for sustainable development: A comparative study of india and china. *Materials Today: Proceedings*. <https://doi.org/https://doi.org/10.1016/j.matpr.2021.09.242>
- Sidek, M. H. M., Azis, N., Hasan, W. Z. W., Ab Kadir, M. Z. A., Shafie, S., & Radzi, M. A. M. (2017, 2017/04/01/). Automated positioning dual-axis solar tracking system with precision elevation and azimuth angle control. *Energy*, 124, 160-170. <https://doi.org/https://doi.org/10.1016/j.energy.2017.02.001>
- Singh, R., Kumar, S., Gehlot, A., & Pachauri, R. (2018). An imperative role of sun trackers in photovoltaic technology: A review. *Renewable and Sustainable Energy Reviews*, 82, 3263-3278.
- Soulayman, S., Hamoud, M., Hababa, M. A., & Sabbagh, W. (2021). Feasibility of Solar Tracking System for PV Panel in Sunbelt Region. *Journal of Modern Power Systems and Clean Energy*, 9(2), 395-403. <https://doi.org/10.35833/MPCE.2018.000658>

- Su, Y., Zhang, Y., & Shu, L. (2018). Experimental study of using phase change material cooling in a solar tracking concentrated photovoltaic-thermal system. *Solar Energy*, *159*, 777-785.
- Suki, N. M., Suki, N. M., Sharif, A., Afshan, S., & Jermisittiparsert, K. (2022, 2022/01/01/). The role of technology innovation and renewable energy in reducing environmental degradation in Malaysia: A step towards sustainable environment. *Renewable Energy*, *182*, 245-253. <https://doi.org/https://doi.org/10.1016/j.renene.2021.10.007>
- Tan, M.-H., Wang, T.-K., Wong, C.-W., Lim, B.-H., Yew, T.-K., Tan, W.-C., Lai, A.-C., & Chong, K.-K. (2019, 2019/02/01/). Optimization Study of Parasitic Energy Losses in Photovoltaic System with Dual-Axis Solar Tracker Located at Different Latitudes. *Energy Procedia*, *158*, 302-308. <https://doi.org/https://doi.org/10.1016/j.egypro.2019.01.093>
- Yang, D., Dong, Z., Lim, L. H. I., & Liu, L. (2017, 2017/09/01/). Analyzing big time series data in solar engineering using features and PCA. *Solar Energy*, *153*, 317-328. <https://doi.org/https://doi.org/10.1016/j.solener.2017.05.072>
- Yilmaz, S., Ozcalik, H. R., Dogmus, O., Dincer, F., Akgol, O., & Karaaslan, M. (2015). Design of two axes sun tracking controller with analytically solar radiation calculations. *Renewable and Sustainable Energy Reviews*, *43*, 997-1005.
- Yu, Q., Zhao, H., Zhao, H., Sun, S., Ji, X., Li, M., & Wang, Y. (2019, 2019/01/01/). Preparation of tobacco-stem activated carbon from using response surface methodology and its application for water vapor adsorption in solar drying system. *Solar Energy*, *177*, 324-336. <https://doi.org/https://doi.org/10.1016/j.solener.2018.11.029>



© 2022. The Authors. This article is an open access article distributed under the terms and conditions of the Creative Commons Attribution-ShareAlike 4.0 (CC BY-SA) International License (<http://creativecommons.org/licenses/by-sa/4.0/>)